JACS
JOURNAL OF THE AMERICAN CHEMICAL SOCIETY

Communication

pubs.acs.org/JACS

Freezing and Melting of Salt Hydrates Next to Solid Surfaces Probed by Infrared–Visible Sum Frequency Generation Spectroscopy

Emmanuel Anim-Danso, Yu Zhang, and Ali Dhinojwala*

Department of Polymer Science, The University of Akron, Akron, Ohio 44325-3909, United States

Supporting Information

ABSTRACT: Understanding the freezing of salt solutions near solid surfaces is important in many scientific fields. Here we use sum frequency generation (SFG) spectroscopy to study the freezing of a NaCl solution next to a sapphire substrate. During cooling we observe two transitions. The first corresponds to segregation of concentrated brine next to the sapphire surface as we cool the system down to the region where ice and brine phases coexist. At this transition, the intensity of the ice-like peak decreases, suggesting the disruption of hydrogen-bonding by sodium ions. The second transition corresponds to the formation of NaCl hydrates with abrupt changes in both the SFG intensity and the sharpness of spectral peaks. The similarity in the position of the SFG peaks with those observed using IR and Raman spectroscopy indicates the formation of $NaCl{\cdot}2H_2O$ crystals next to the sapphire substrate. The melting temperatures of the hydrates are very similar to those reported for bulk $NaCl{\cdot}2H_2O$. This study enhances our understanding of nucleation and freezing of salt solutions on solid surfaces and the effects of salt ions on the structure of interfacial ice.

Salt and water interactions are of great significance to climatology, geology, biology, and many other fields of science. For example, hydrated NaCl particles are better nuclei for cloud formation than non-hydrated salt particles.[1,2] Ozone depletion in the stratosphere has been linked to interactions of nitric acid salts with ice.[3] Magnesium sulfate hydrates found within the saline deposits on Mars provided information on the history of water on Mars.[4] In geology, identifying the salinity of various fluid inclusions can lead to greater understanding of diagenesis, metamorphism, and hydrothermal processes.[5,6] The formation of salt hydrate clusters was studied using infrared (IR)[7−9] and Raman spectroscopy.[6,10] Frequency shifts and the absorption strength of the O−H stretching vibrations observed in the IR measurements were used to study the nature or strength of hydrogen-bonds,[9,11] and IR spectroscopy was used to measure the relaxation time of O−H stretching in NaCl hydrate to study the behavior of confined water.[12] Raman spectroscopy was used extensively to study fluid inclusions in minerals and rock formations.[5,6,10,13−16]

Although many studies have enumerated the importance of studying the freezing of salt solutions near surfaces, there is no direct experimental measurement of hydrates freezing near solid surfaces.[3,17] Here, we report for the first time the use of IR–visible sum frequency generation (SFG) spectroscopy to study the freezing of salt solutions next to sapphire substrates. Sapphire is a model substrate for studying geochemical[18] and catalytic processes,[19] is transparent in visible and IR spectral regions, and serves as a good substrate for SFG measurements. We observe the segregation of salt solution in the region where ice and brine phases coexist and subsequent freezing of NaCl hydrates next to sapphire substrates. The positions of the hydrate peaks in the SFG spectra of the surface hydrates are similar to those found for NaCl dihydrate crystals using IR and Raman spectroscopy. The similarities in the melting transition temperatures suggest that the concentration of NaCl salt solutions in contact with sapphire substrates before freezing must be similar to the eutectic concentration of NaCl salt solution. We believe that this study increases our understanding of the influence of solid surfaces on the nucleation and freezing of salt solutions and the effect of salt ions on the structure of interfacial ice.

The use of SFG to study aqueous and nonaqueous interfaces was described previously.[20−22] Recently, we described a sample cell to study the freezing of ice using sapphire prisms in total internal reflection geometry (Figure S1, Supporting Information).[23,24] The sapphire prisms were cleaned using a procedure described in previous publications.[24−26] The cleaning procedure was verified by using X-ray photon spectroscopy and collecting SFG spectra of blank sapphire prisms to make sure there were no hydrocarbon signals. Ultrapure water from a Millipore filtration system (with deionizing and organic removal columns) with a resistivity of 18.2 MΩ·cm was used to make 0.1 M NaCl (purity ≥99.0%, purchased from Fisher Scientific) solution. The salt solution was then injected into a sample cell and cooled using a temperature stage described previously.[24] The temperatures were changed using a 4 °C/min cooling or heating rate, with a 30 min equilibration time before collecting the SFG spectra. An effective heating rate of 0.033 °C/min was used to measure the melting temperatures.

Figure 1 shows the SFG spectra collected during the cooling of 0.1 M NaCl solution in contact with a sapphire substrate using SSP and PPP polarizations. The SSP and PPP polarizations provide complementary information and could be useful in interpreting the orientation of molecules. For the salt solution in the liquid state (empty squares), three main peaks are observed, at 3200, 3450, and 3720 cm^{-1}. The peak at 3720 cm^{-1} is assigned to hydroxyl groups on the sapphire surface.[24,25,27] The peaks at 3200 and 3450 cm^{-1} are attributed to strongly tetrahedrally coordinated (ice-like) and lower coordination (liquid-like)

Received: April 12, 2013
Published: May 22, 2013

   dx.doi.org/10.1021/ja403437c | J. Am. Chem. Soc. 2013, 135, 8496−8499

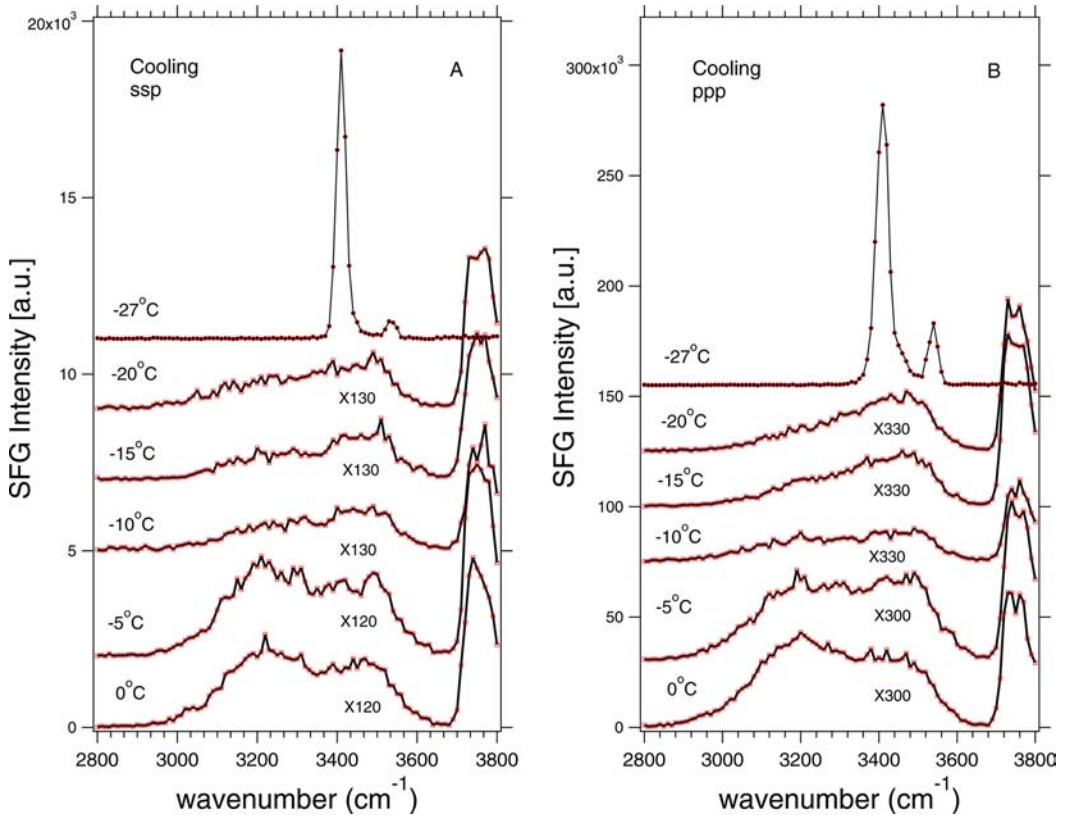

Figure 1. SFG spectra collected in SSP (A) and PPP (B) polarizations during the cooling cycle. The empty squares and filled circles correspond to temperatures where salt solution and NaCl hydrate, respectively, are in contact with the sapphire substrate. The solid lines joining the data points are provided as a guide. The data were also fitted using the Lorentzian equation, and the fitting results are summarized in the Supporting Information (Figure S2; Tables S1 and S2). The freezing transition temperatures for the hydrate formation are between −25 and −30 °C.

hydrogen-bond stretches, respectively.[28,29] However, alternate assignments for the hydrogen-bonded region were discussed recently in the literature.[30−33] The SFG spectra of 0.1 M NaCl solution show a stronger ice-like peak at 3200 cm^{-1} in comparison to the liquid-like peak at 3450 cm^{-1}. For spectra collected at −10 °C, the ratio of ice-like and liquid-like peaks changes, and the SFG intensity drops (Figure 1). Upon further cooling, we observe a very sharp peak near 3410 cm^{-1}. This sudden change in structure indicates crystallization of hydrates.

Table 1 summarizes the assignments for NaCl dihydrate crystals using IR and Raman spectroscopy. There are four main peaks observed, at 3530−3540, 3430−3440, 3420−3425, and 3405 cm^{-1}. These peaks correspond to four different positions of OH groups in the hydrate crystals, and the magnitudes of these peaks in IR spectroscopy are related to the composition and type of crystal structure.[34] The peak positions determined after fitting the SFG spectra using a Lorentzian function are also summarized in Table 1. There is one dominant peak at 3410 cm^{-1}, with spectral widths of 10 and 14 cm^{-1} in SSP and PPP polarizations, respectively. The second, smaller peak is at 3530 cm^{-1}, with SSP and PPP spectral widths both of 10 cm^{-1}. The resolution of these hydrate peaks is limited by the resolution of the IR laser and the SFG spectrometer (8−10 cm^{-1}) used in these experiments. The narrow spectral width and the similarity in the spectral signatures between IR, Raman, and SFG spectroscopy indicate the formation of NaCl dihydrate crystals next to sapphire substrates.

Table 1. Comparison of NaCl Dihydrate Peak Assignments for IR,[8] Raman,[10] and SFG Spectroscopy (cm^{-1})

temp (°C)	SFG	IR	Raman
−170[8,10]		3531	3536
		3433	3438
		3423	3422
		3413	3406
−27	3530 (SSP)		
	3410 (SSP)		
	3530 (PPP)		
	3410 (PPP)		
−26[8]		3537	
		3425	

To measure the melting transition temperature of the NaCl dihydrate crystals, we heated the frozen sample at a heating rate of 0.033 °C/min. Interestingly, around −23 °C (for both polarizations, see Figure 2), we observed a decrease in the hydrate signal intensity, suggesting a pre-melting layer or possibly a loosening of the hydrogen-bonding network in the hydrate crystals before the melting transition. When the temperature was increased further by only 1 °C, the hydrate crystals melted (−22 °C), showing the previously observed water peaks in the cooling experiments. The melting temperature is similar to the eutectic temperature of bulk NaCl dihydrate crystals, at −21.2 °C.

Interestingly, we observe no ice peak at 3150 cm^{-1} as one would expect upon heating and freezing ice adjacent to a sapphire substrate.[24] Additionally, the spectral features shifted dramatically near −10 °C in the cooling cycle. These observations suggest that the sample starts out with a uniform 0.1 M (0.6% NaCl) concentration of salt solution. As we cool the salt solution,

dx.doi.org/10.1021/ja403437c | J. Am. Chem. Soc. 2013, 135, 8496−8499

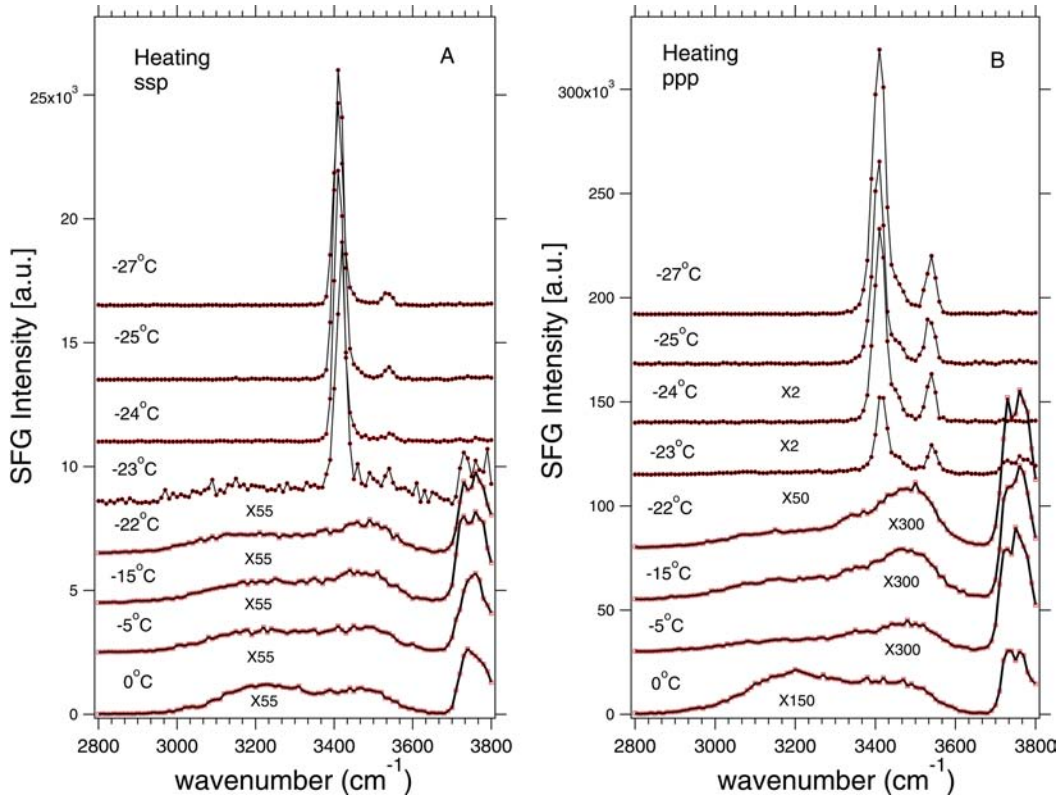

Figure 2. SFG spectra collected in SSP (A) and PPP (B) polarizations during the heating cycle. The empty squares and filled circles correspond to temperature where salt solution and NaCl hydrate, respectively, are in contact with the sapphire substrate. The solid lines joining the data points are provided as a guide. The data were also fitted using the Lorentzian equation, and the fitting results are summarized in the Supporting Information (Figure S3; Tables S3 and S4). The melting transition temperature for hydrate formation is −22 °C.

we cross the phase boundary shown in the phase diagram of NaCl solution in Figure 3.[35] This results in the freezing of ice and the formation of brine which is more concentrated than in the original salt solution at −10 °C. The concentrated brine is segregated next to the sapphire interface; thus, no ice peak is observed in the SFG spectra. This may be analogous to the freezing of water on the surface of the Antarctic Ocean and the cascade of higher-density brine pushed down toward the ocean floor. For our system, the segregation of brine next to the sapphire substrate is driven by surface effects rather than gravity. As we lower the temperature below −10 °C, we expect the salt concentration to increase and to follow the phase diagram (indicated by the arrows in Figure 3) as more water molecules are incorporated in the growing ice crystals. Eventually, the salt concentration will reach the eutectic concentration, and the solution will crystallize to form hydrates. The freezing point of the hydrate crystals in our experiment is ∼6 °C lower than the transition reported from bulk measurements (−21.2 °C). Using mass conservation, we estimate that the thickness of the brine layer next to the sapphire substrate is $\sim c_i t_c / c_e$, where c_i, t_c, and c_e are the initial brine concentration, the thickness of the sample cell (0.04 cm), and the concentration at the eutectic point, respectively. We estimate that there is ∼10 μm thick layer of brine next to the sapphire substrate at the eutectic point, and the ice layer is considerably thicker than the concentrated brine layer. During the heating cycle, we observed pre-melting around 1 °C before the actual melting transition of hydrate crystals at −22 °C. Immediately after melting, we expect the salt concentration to be near the eutectic concentration and then continue to decrease as we heat the solution (corresponding to the arrows on the phase diagram). The SFG spectrum collected at 0 °C during the heating cycle recovers back to the spectrum that we obtained before the cooling cycle, indicating that the ice melted upon heating and the solution concentration next to the sapphire substrate returned to the starting concentration, 0.1 M NaCl.

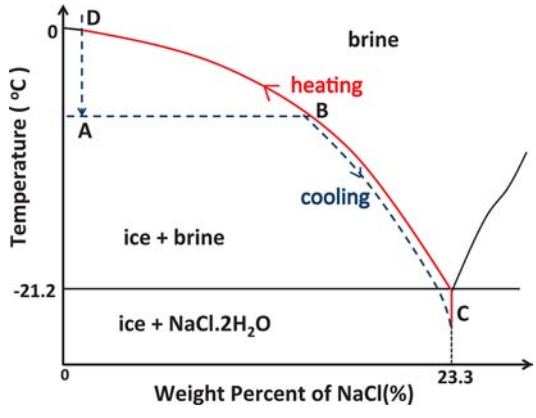

Figure 3. Phase diagram of NaCl solution reconstructed from *CRC Handbook*.[35] In the SFG experiments the salt solution was cooled below 0 °C, following the blue dashed line. Near −10 °C (point A) the ice freezes, and we expect an increase in the concentration of brine (point B). As the temperature is decreased further, the concentration of NaCl increases, as indicated by the blue dashed lines, until the eutectic point is reached. The hydrate freezes around 6 °C, below the temperature expected for bulk freezing of hydrates (point C). On heating, the path is reversed, and the hydrates melt between −23 and −22 °C. Finally, the ice melts near 0 °C (point D).

dx.doi.org/10.1021/ja403437c | *J. Am. Chem. Soc.* 2013, 135, 8496−8499

The use of NaCl solution in cooling and heating experiments allows us to study the effect of salt concentration on water structure at the sapphire surface. In the phase region that corresponds to the coexistence of ice and brine, the temperature can be related to the change in the concentration of the brine in contact with the sapphire substrate. After transition to the coexistence curve, there is a shift in the SFG peaks and a strong attenuation of the SFG signals. Attenuation of the SFG signal in the salt solution was already observed at solid surfaces[36,37] and explained to be due to the formation of the double layer that screens the surface charge.[38] For concentrated brine there is a decrease in intensity of the 3200 cm^{-1} peak, while the 3450 cm^{-1} peak increases in intensity. This could be attributed to the presence of sodium ions at the interface.[39,40]

These experimental results raise some very interesting questions. The relative intensities of various hydrate peaks in the IR and Raman spectra are characteristic of the crystal structure. However, the selection rules of SFG are different from those of IR and Raman spectroscopy, and the intensity of the SFG signals depends on the orientation of the molecules. The microscopic susceptibility of the four hydrate sites and their relative orientation with respect to the surface need to be understood before interpreting the ratio of the different hydrate peaks in the SFG spectra. Additionally, the pre-melting layer observed here suggests the intriguing possibility that the surface transition temperatures could be different from those in the bulk.

■ ASSOCIATED CONTENT

Supporting Information

Cleaning procedure, experimental setup, and results of fits. This material is available free of charge via the Internet at http://pubs.acs.org.

■ AUTHOR INFORMATION

Corresponding Author

ali4@uakron.edu

Notes

The authors declare no competing financial interest.

■ ACKNOWLEDGMENTS

The authors thank Edward Laughlin, Anish Kurian, and Liehui Ge for their help in designing the temperature stage. We also thank Yeneneh Yimer, Gary Leuty, and Mike Heiber for helpful discussions. This work was supported by NSF-DMR GOALI Grant. We also thank GE Global Research for providing support to fund the design of the temperature cell for SFG.

■ REFERENCES

(1) Abbatt, J.; Benz, S.; Cziczo, D.; Kanji, Z.; Lohmann, U.; Möhler, O. *Science* **2006**, *313*, 1770.

(2) Wise, M. E.; Baustian, K. J.; Koop, T.; Freedman, M. A.; Jensen, E. J.; Tolbert, M. A. *Atmos. Chem. Phys.* **2012**, *12*, 1121.

(3) Bartels-Rausch, T. *Nature* **2013**, *494*, 27.

(4) Vaniman, D. T.; Bish, D. L.; Chipera, S. J.; Fialips, C. I.; Carey, J. W.; Feldman, W. C. *Nature* **2004**, *431*, 663.

(5) Roedder, E. *Rev. Mineral.* **1984**, *12*, 305.

(6) Baumgartner, M.; Bakker, R. J. *Mineral. Petrol.* **2009**, *95*, 1.

(7) Lucchesi, P. J.; Glasson, W. A. *J. Am. Chem. Soc.* **1956**, *78*, 1347.

(8) Franks, F. *Water: A comprehensive treatise. Vol. 2. Water in crystalline hydrates: aqueous solutions of simple nonelectrolytes*; Plenum: New York, 1973.

(9) Lutz, H. *Bonding and structure of water molecules in solid hydrates. Correlation of spectroscopic and structural data*; Springer: Berlin, 1988; pp 97−125.

(10) Dubessy, J.; Audeoud, D.; Wilkins, R.; Kosztolanyi, C. *Chem. Geol.* **1982**, *37*, 137.

(11) Lutz, H. D.; Jung, C. *J. Mol. Struct.* **1997**, *404*, 63 .

(12) Pandelov, S.; Pilles, B. M.; Werhahn, J. C.; Iglev, H. *J. Phys. Chem. A* **2009**, *113*, 10184.

(13) Samson, I. M.; Walker, R. T. *Can. Mineral.* **2000**, *38*, 35.

(14) Bakker, R. J. *Can. Mineral.* **2004**, *42*, 1283.

(15) Baumgartner, M.; Bakker, R. J. *Chem. Geol.* **2010**, *275*, 58 .

(16) Ni, P.; Ding, J.; Rao, B. *Chin. Sci. Bull.* **2006**, *51*, 108.

(17) Bartels-Rausch, T.; Bergeron, V.; Cartwright, J. H. E.; Escribano, R.; Finney, J. L.; Grothe, H.; Gutierrez, P. J.; Haapala, J.; Kuhs, W. F.; Pettersson, J. B. C.; Price, S. D.; Sainz-Diaz, C. I.; Stokes, D. J.; Strazzulla, G.; Thomson, E. S. *Rev. Mod. Phys.* **2012**, *84*, 885.

(18) Stumm, W. *Chemistry of the Solid-Water Interface: Processes at the Mineral-Water and Particle-Water Interface in Natural Systems*; Wiley: New York, 1992.

(19) Sormorjai, G. A. *Introduction to Surface Chemistry and Catalysis*; Wiley: New York, 1994.

(20) Shen, Y. R. *The Principles of Nonlinear Optics*; Wiley: New York, 1984.

(21) Hsu, P. Y.; Dhinojwala, A. *Langmuir* **2012**, *28*, 2567.

(22) Nanjundiah, K.; Hsu, P. Y.; Dhinojwala, A. *J. Chem. Phys.* **2009**, *130*, 024702.

(23) Gautam, K. S.; Schwab, A. D.; Dhinojwala, A.; Zhang, D.; Dougal, S. M.; Yeganeh, M. S. *Phys. Rev. Lett.* **2000**, *85*, 3854.

(24) Anim-Danso, E.; Zhang, Y.; Alizadeh, A.; Dhinojwala, A. *J. Am. Chem. Soc.* **2013**, *135*, 2734.

(25) Zhang, L.; Tian, C.; Waychunas, G. A.; Shen, Y. R. *J. Am. Chem. Soc.* **2008**, *130*, 7686.

(26) Lützenkirchen, J.; Zimmermann, R.; Preocanin, T.; Filby, A.; Kupcik, T.; Küttner, D.; Abdelmonem, A.; Schild, D.; Rabung, T.; Plaschke, M.; Brandenstein, F.; Werner, C.; Geckeis, H. *Adv. Colloid Interface Sci.* **2010**, *157*, 61.

(27) Sung, J.; Shen, Y. R.; Waychunas, G. A. *J. Phys.: Condens. Matter* **2012**, *24*, 124101.

(28) Shen, Y. R.; Ostroverchov, V. *Chem. Rev.* **2006**, *94*, 1140.

(29) Du, Q.; Freysz, E.; Shen, Y. R. *Phys. Rev. Lett.* **1994**, *72*, 238.

(30) Sovago, M.; Campen, R. K.; Wurpel, G. W. H.; Müller, M.; Bakker, H. J.; Bonn, M. *Phys. Rev. Lett.* **2008**, *100*, 173901.

(31) Walker, D. S.; Hore, D. K.; Richmond, G. L. *J. Phys. Chem. B* **2006**, *110*, 20451.

(32) Gan, W.; Wu, D.; Zhang, Z.; ran Feng, R.; fei Wang, H. *J. Chem. Phys.* **2006**, *124*, 114705.

(33) Skinner, J. L.; Pieniazek, P. A.; Gruenbaum, S. M. *Acc. Chem. Res.* **2012**, *45*, 93.

(34) Klewe, B.; Pedersen, B. *Acta Crystallogr. Sect. B* **1974**, *30*, 2363.

(35) Lide, D. R., Ed. *CRC Handbook of Chemistry and Physics*, 86th ed.; CRC Press: Boca Raton, 2005; pp 8−71.

(36) Jena, K. C.; Covert, P. A.; Hore, D. K. *J. Phys. Chem. Lett.* **2011**, *2*, 1056.

(37) Flores, S. C.; Kherb, J.; Konelick, N.; Chen, X.; Cremer, P. S. *J. Phys. Chem. C* **2012**, *116*, 5730.

(38) Adamson, A. W.; Gast, A. P. *Physical chemistry of surfaces*; Wiley: New York, 1997.

(39) Hribar, B.; Southall, N. T.; Vlachy, V.; Dill, K. A. *J. Am. Chem. Soc.* **2002**, *124*, 12302.

(40) Nihonyanagi, S.; Yamaguchi, S.; Tahara, T. *J. Am. Chem. Soc.* **2010**, *132*, 6867.